Multiple Chiral Doublet Bands of Identical Configuration in ^{103}Rh

I. Kuti,[1] Q. B. Chen,[2] J. Timár,[1] D. Sohler,[1] S. Q. Zhang,[2] Z. H. Zhang,[2] P. W. Zhao,[2] J. Meng,[2] K. Starosta,[3] T. Koike,[4] E. S. Paul,[5] D. B. Fossan,[6] and C. Vaman[6]

[1]*Institute for Nuclear Research, Hungarian Academy of Sciences, Pf. 51, 4001 Debrecen, Hungary*
[2]*State Key Laboratory of Physics and Technology, School of Physics, Peking University, Beijing 100871, China*
[3]*Department of Chemistry, Simon Fraser University, Burnaby, British Columbia V5A 1S6, Canada*
[4]*Graduate School of Science, Tohoku University, Sendai 980-8578, Japan*
[5]*Oliver Lodge Laboratory, University of Liverpool, Liverpool L69 7ZE, United Kingdom*
[6]*Department of Physics and Astronomy, State University of New York, Stony Brook, New York 11794-3800, USA*

(Received 23 April 2014; published 14 July 2014)

Three sets of chiral doublet band structures have been identified in the ^{103}Rh nucleus. The properties of the observed chiral doublet bands are in good agreement with theoretical results obtained using constrained covariant density functional theory and particle rotor model calculations. Two of them belong to an identical configuration and provide the first experimental evidence for a novel type of multiple chiral doublets, where an "excited" chiral doublet of a configuration is seen together with the "yrast" one. This observation shows that the chiral geometry in nuclei can be robust against the increase of the intrinsic excitation energy.

DOI: 10.1103/PhysRevLett.113.032501 PACS numbers: 21.10.Hw, 21.10.Re, 21.60.-n, 23.20.Lv

A novel form of spontaneous symmetry breaking, the chiral rotation of triaxial nuclei, was suggested in 1997 [1]. It was shown that in special circumstances, referred to as chiral geometry, in the intrinsic frame of the rotating triaxial nucleus the total angular momentum vector lies outside the three principal planes. Thus, its components along the principal axes can be oriented in left- and right-handed ways. In the laboratory frame, the chiral symmetry is restored, which manifests itself as a pair of $\Delta I = 1$ nearly degenerate bands with the same parity. Such chiral doublet bands were first identified in four $N = 75$ isotones in 2001 [2]. So far, many chiral candidate nuclei have been reported experimentally in the $A \sim 80$, 100, 130, and 190 mass regions [3–21]. Besides the simplest chiral configurations composed of one unpaired proton and neutron, composite chiral configurations, containing more than one unpaired protons and/or neutrons, have also been observed in the odd-mass or even-even neighbors of the odd-odd chiral nuclei [10,18]. These observations show that chirality is not restricted to a certain configuration in a mass region; i.e., the chiral geometry can be robust against the change of configuration. It was even demonstrated recently by Meng *et al.* [22–25], based on adiabatic and configuration-fixed constrained triaxial covariant density functional theory (CDFT) calculations, that it is possible to have multiple pairs of chiral doublet bands in a single nucleus, and the acronym MχD was introduced for this phenomenon. The first experimental evidence for the predicted MχD was reported in ^{133}Ce [26] and also possibly in ^{107}Ag [27].

It is also interesting to study the robustness of chiral geometry against the increase of the intrinsic excitation energy, i.e., if the chiral geometry is sustained in the higher-lying bands of a certain chiral configuration. In all the known cases, the chiral doublet corresponds to the two lowest-lying bands of a configuration. Even for MχD in ^{133}Ce [26] and ^{107}Ag [27], each chiral doublet structure corresponds to two lowest-lying bands with a distinct configuration. Therefore, study of the third and forth bands of the same chiral configuration is needed to answer the question of the investigated robustness. Very recent model calculations predicted multiple chiral doublet bands that belong to the same configuration [28–30]. In this Letter, we report on the first experimental evidence for such a type of MχD in the ^{103}Rh nucleus.

Medium- and high-spin states of ^{103}Rh were populated using the ^{96}Zr(^{11}B, $4n$) reaction at a beam energy of 40 MeV. The beam, provided by the 88-inch cyclotron of the LBNL, impinged upon an enriched 500 μg/cm^2 thick self-supporting Zr foil. The emitted γ-rays were detected by the Gammasphere spectrometer. Approximately 9×10^8 four- and higher-fold events were accumulated and sorted off-line into two-dimensional and three-dimensional histograms. The data analysis was carried out using the RADWARE software package [31]. A more complete level scheme of ^{103}Rh was constructed using the observed coincidence relations and relative intensities of the gamma transitions and based on the formerly reported states [19,32]. Spin assignments for the new states were deduced from the measurements of angular-intensity ratios, based on the method of directional correlation from oriented states (DCO) [33]. The parities were deduced using the additional assumption that if a level decays to a band by both quadrupole and dipole transitions with comparable intensities, then the quadrupole transition is $E2$ and the dipole is

 © 2014 American Physical Society

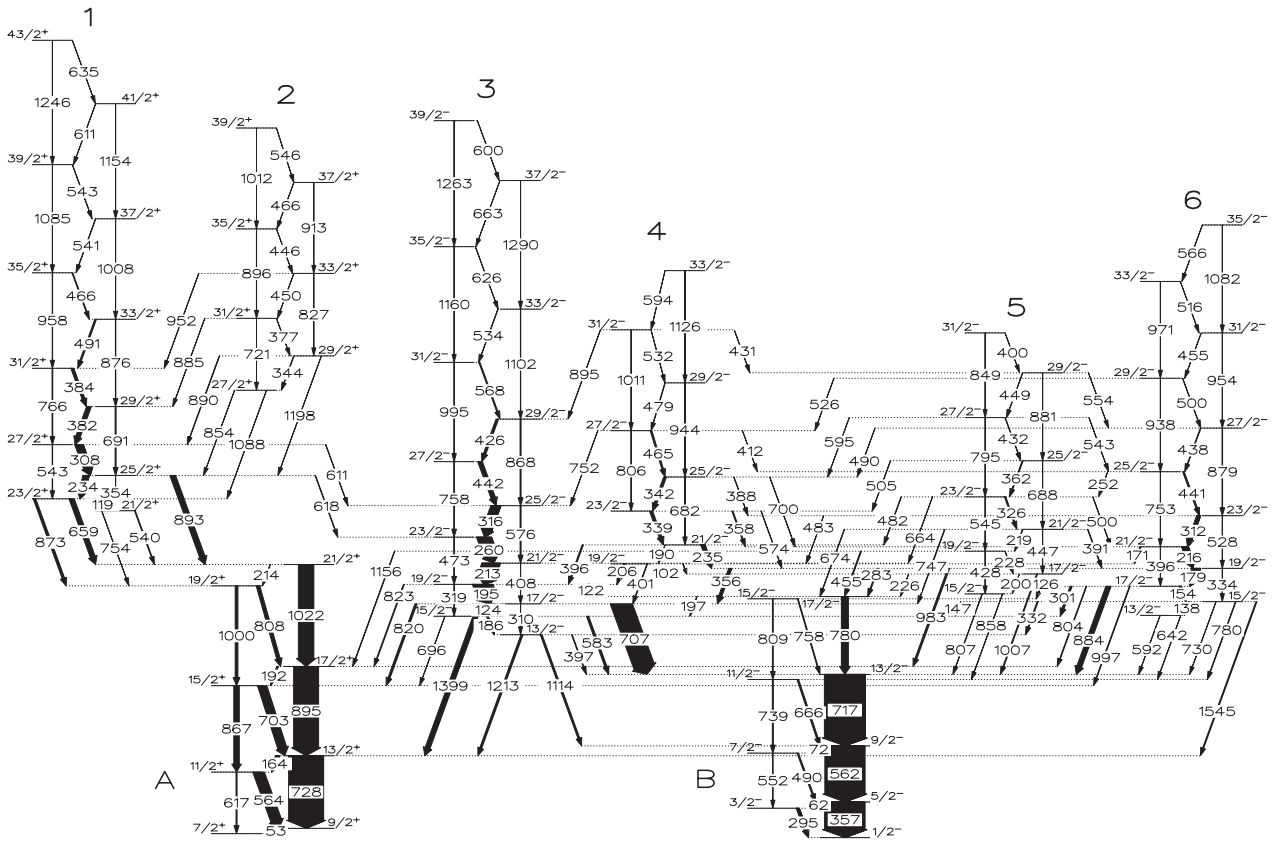

FIG. 1. Partial level scheme of ^{103}Rh. The energies are given in keV, and the widths of the arrows are proportional to the relative transition intensities.

$M1$. Several new rotational bands have been found, and the previously reported ones were extended to higher spins. A partial level scheme showing the bands relevant to the focus of this Letter is plotted in Fig. 1. Bands A and B were formerly reported in Ref. [32], while bands 1 and 2 were identified earlier and assigned as a chiral doublet with configuration $\pi(g_{9/2}) \otimes \nu(h_{11/2})^2$ in Ref. [19]. Bands 3 and 6 were first reported in Ref. [32] up to spins 29/2 and 25/2, respectively, with a tentative configuration assignment of $\pi(g_{9/2})^2(p_{1/2})$. In the present work, we extended these bands to spins 39/2 and 35/2, respectively. Two of the newly observed bands, labeled as bands 4 and 5, are presented in Fig. 1. Figure 2 shows triple-coincidence γ-ray spectra proving the placements of the levels in bands 4 and 5, with the in-band transitions highlighted. For these bands, the spin parities were deduced from DCO measurements. In the present geometry, setting the gate on a stretched quadrupole transition, R_{DCO} values of ~1.0 and ~0.5 were expected for stretched quadrupole and stretched dipole transitions, respectively. An $E2$ electromagnetic character to the 674- and 1007 keV transitions linking band 5 to band B was assigned based on the DCO values of 0.93(11) and 1.07(4), respectively, setting the gate on the 717 keV $E2$ transition of band B. Similarly the 574 and 700 keV transitions linking band 4 to band 6 are considered to have $E2$ character, based on the DCO values of 0.89(18) and 0.88 (19) obtained by gating on the 884 keV $E2$ transition linking band 6 to band B. These quadrupole transitions fix the negative parity and the spins for bands 4 and 5. This assignment is verified by the 0.55(2) and 0.54(13) DCO values of the 396 and 391 keV stretched $M1$ transitions linking band 4 to band 3 and band 5 to band 6, respectively.

The $\Delta I = 1$ bands 3–6 all have negative parity and are linked to each other by many transitions. Furthermore, the energy differences between the same-spin levels are rather small; for bands 3 and 4 these values are about 300 keV and for bands 6 and 5 about 100 keV, and their $B(M1)/B(E2)$ values are very similar. These properties may indicate

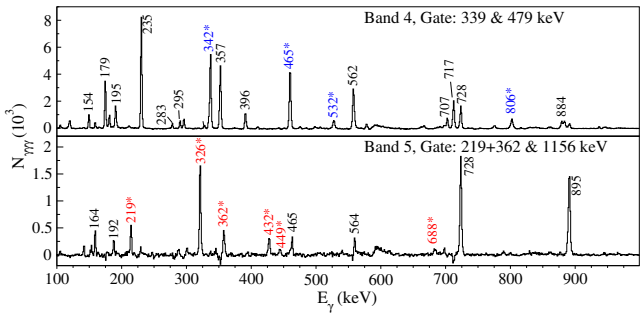

FIG. 2 (color online). Typical $\gamma\gamma\gamma$-coincidence spectra obtained in the present work showing the placement of the γ rays in bands 4 and 5. Transitions marked with stars and labeled in blue or red are in-band transitions.

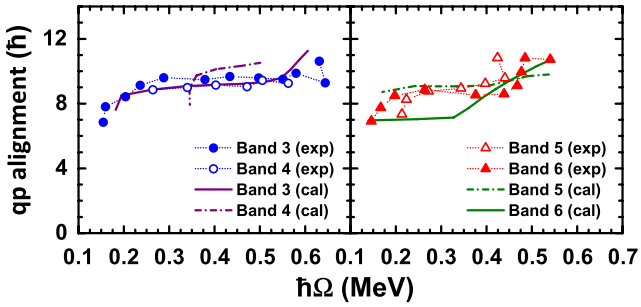

FIG. 3 (color online). Quasiparticle alignments of bands 3–6. For details, see the text.

chirality. Indeed, in neighboring ^{105}Rh, similar structures of three $\Delta I = 1$ bands have been observed and identified tentatively as the three lowest-energy bands of the $\pi g_{9/2} \otimes \nu h_{11/2}(g_{7/2}, d_{5/2})$ configuration [17]. In ^{105}Rh, the lowest-energy one of the three bands is thought to have planar geometry, while the two higher-energy bands are considered as a chiral doublet. In ^{103}Rh, we see four bands that could correspond to two chiral doublets. To assist in the comparison of the properties of bands 3–6, we have derived their quasiparticle alignments as defined in Ref. [34]. $K = 1/2$ and the $\mathcal{J}_0 = 7\hbar^2/\mathrm{MeV}$ and $\mathcal{J}_1 = 15.7\hbar^4/\mathrm{MeV}^3$ parameters of the Harris formula $\mathcal{J} = \mathcal{J}_0 + \mathcal{J}_1\omega^2$, describing the dependence of moments of inertia on the rotational frequency, have been adopted in the derivation. The obtained alignments are shown in Fig. 3. Although the alignment value is $\sim 9\hbar$ for all four bands in a wide interval of rotational frequency, there is a pronounced similarity between bands 3 and 4 and also between bands 5 and 6. These similarities enable us to group the four bands into two possible chiral doublets. According to this grouping, the lowest-energy and the second-lowest-energy bands (bands 3 and 4, respectively) could form the "yrast" chiral doublet, while the next two bands in energy (bands 6 and 5) could form the "excited" chiral doublet of the probable $\pi g_{9/2} \otimes \nu h_{11/2}(g_{7/2}, d_{5/2})$ configuration. We need to mention, however, that bands 4 and 6 are so close to each other in energy that their energy ordering varies with spin.

In order to understand the nature of the observed band structure in ^{103}Rh, adiabatic and configuration-fixed constrained CDFT calculations [22] were first performed to search for the possible configurations and deformations. Subsequently, the configurations and deformations were further confirmed and reexamined by tilted axis cranking CDFT (TAC-CDFT) calculations [35–38] determining the energy spectra, Routhians, spin-frequency relations, deformations, and alignments. Finally, with the obtained configurations and deformations, quantum particle rotor model [26,39,40] calculations were performed to study the energy spectra and $B(M1)/B(E2)$ ratios for both the positive- and the negative-parity bands.

The potential-energy surface in the β-γ plane obtained from the CDFT calculations with effective interaction PC-PK1 [41] shows that the ground state of ^{103}Rh has a triaxial deformation with a quadrupole deformation of $\beta = 0.25$ and a triaxiality parameter of $\gamma = 20°$ and is soft with respect to the γ degree of freedom. The configuration-fixed calculations provided the $\pi(1g_{9/2})^{-1}$ (more precisely, seven protons in $g_{9/2}$ shell) and the $\pi(2p_{1/2})^1$ unpaired-nucleon configurations for bands A and B, in good agreement with previous configuration assignments [32]. Among the five lowest-lying configurations with three unpaired nucleons, one positive-parity and four negative-parity configurations have been found. The band head of the positive-parity $\pi(1g_{9/2})^{-1} \otimes \nu(1h_{11/2})^2$ configuration is predicted to have a triaxial shape of $\beta = 0.29$, $\gamma = 11.0°$. Two of the four negative-parity bands are predicted to have triaxial shape, namely, configuration $\pi(1g_{9/2})^{-1} \otimes \nu(1h_{11/2})^1(2d_{5/2})^1$ with $\beta = 0.27$, $\gamma = 18.7°$ and configuration $\pi(1g_{9/2})^{-1} \otimes \nu(1h_{11/2})^1(1g_{7/2})^{-1}$ with $\beta = 0.26$, $\gamma = 14.5°$. Here $(g_{7/2})^{-1}$ denotes the occupation of five neutrons in the $g_{7/2}$ shell.

In order to study the rotational behavior of the predicted configurations, and to reexamine their configurations and deformations with rotation, TAC-CDFT [35–38] with the effective interaction PC-PK1 [41] was adopted. Due to the strong mixing between low-j orbits, we kept the configurations of the high-j valence nucleons fixed and left the other nucleons automatically occupying the lowest levels. For positive-parity bands, we fixed the high-j orbitals $\pi(1g_{9/2})^{-1} \otimes \nu(1h_{11/2})^2$, while for negative-parity bands we fixed the $\pi(1g_{9/2})^{-1} \otimes \nu(1h_{11/2})^1$. The calculated energies as a function of spin as well as the Routhians and spins as a function of the rotational frequency for the above two configurations are in a good agreement with the experimental values for bands 1,2 and 3–6, respectively. With increasing rotational frequency, the β shape parameter was found to decrease somewhat, while the γ parameter increased to around 30° with average values of 20° in the observed frequency range. For the low-j components of the negative-parity configuration, a $g_{7/2}$ neutron is found to contribute a large alignment along the short axis (about $3\hbar$) in the TAC-CDFT calculations and the contribution from other $g_{7/2}$ neutrons can be regarded as a part of the core. Hence, the valence $g_{7/2}$ neutron contributions can be approximated by an effective $(1g_{7/2})^1$ configuration. Therefore, in the following discussions, the configuration for the negative parity bands is written as $\pi g_{9/2}^{-1} \otimes \nu h_{11/2} g_{7/2}^1$. It has also been revealed by the calculations that the angular momenta of the $(1h_{11/2})^1$ and $(1g_{7/2})^1$ neutrons are aligned along the short axis, while the angular momentum of the $(1g_{9/2})^{-1}$ proton is mainly aligned along the long axis, as it is expected in case of chirality. The details will be presented in a forthcoming publication.

In order to study the energy spectra and the $B(M1)/B(E2)$ ratios of the positive- and negative-parity bands, the quantum particle rotor model (PRM) [26,39,40] has been applied for both the $\pi(1g_{9/2})^{-1} \otimes \nu(1h_{11/2})^2$ and $\pi(1g_{9/2})^{-1} \otimes \nu(1h_{11/2})^1(1g_{7/2})^1$ configurations. In the PRM calculations, the input β deformation parameter at the bandhead was $\beta = 0.29$ for the positive parity bands and $\beta = 0.26$ for the negative parity bands. The γ parameter

was adopted as 20°, which was obtained from the TAC-CDFT calculations. The single-j shell Hamiltonian parameter was taken as [42]

$$C = \left(\frac{123}{8}\sqrt{\frac{5}{\pi}}\right)\frac{2N+3}{j(j+1)}A^{-1/3}\beta.$$

For the electromagnetic transitions, the empirical intrinsic quadrupole moment of $Q_0 = (3/\sqrt{5\pi})R_0^2 Z\beta$ with $R_0 = 1.2A^{1/3}$ fm and the gyromagnetic ratios of $g_R = Z/A$, $g_\pi(g_{9/2}) = 1.26$, $g_\nu(h_{11/2}) = -0.21$, $g_\nu(g_{7/2}) = 0.70$ were adopted.

For the two positive-parity bands with the configuration $\pi(1g_{9/2})^{-1} \otimes \nu(1h_{11/2})^2$, a moment of inertia $\mathcal{J}_0 = 23\hbar^2/\mathrm{MeV}$ was used. This was adjusted to reproduce the trend of the energy spectra of bands 1 and 2. The obtained energy spectra are shown in Fig. 4. The PRM results excellently agree with the data. These two bands are separated by ~500 keV at $I = 29/2\hbar$. They approach each other with increasing spin, and the separation finally goes to ~360 keV at $I = 39/2$. The $B(M1)/B(E2)$ values of bands 1 and 2 are similar. The observation that the experimental $B(M1)/B(E2)$ values for bands 1 and 2 do not fall off as quickly with spin as the theoretical values comes from the frozen rotor assumption adopted in PRM. In Ref. [40], a detailed analysis shows that in both ^{103}Rh and ^{105}Rh, the chiral bands with positive parity change from chiral vibration to nearly static chirality at spin $I = 37/2$ and back to another type of chiral vibration at higher spins. Such a conclusion is still held here for the positive-parity doublet.

For the four negative-parity bands of configuration $\pi(1g_{9/2})^{-1} \otimes \nu(1h_{11/2})^1(1g_{7/2})^1$, a moment of inertia of $\mathcal{J}_0 = 25\hbar^2/\mathrm{MeV}$ was adopted. A Coriolis attenuation factor of $\xi = 0.85$ has been employed to take into account the effect of the strong mixing between low-j neutrons. In Fig. 4, the four lowest-energy calculated bands of the above configuration are compared with the experimental bands 3–6. The four calculated bands form two chiral doublets, of which the first one fits the experimental band pair 3 and 4, while the second doublet can also reasonably reproduce the trend of bands 6 and 5. The calculated energies for bands 5 and 6 are higher than the experimental values of about 200 keV, which might be ascribed to the idea that the complex correlations are not fully taken into account in the PRM calculations with single-j shell Hamiltonian. The corresponding calculated electromagnetic transition probabilities, shown in Fig. 4, are also able to reproduce the data reasonably. The weak odd-even $B(M1)/B(E2)$ staggering for bands 3 and 4 is consistent with the case of chiral vibration as discussed in Ref. [43]. For bands 5 and 6, the $B(M1)/B(E2)$ values show a staggering at $I = 15.5\hbar$, which is also reproduced by the PRM.

In contrast with the multiple chiral doublets predicted in Ref. [22] and experimentally reported in ^{133}Ce [26], the observed MχD in the negative-parity bands of ^{103}Rh is built from the first and second doublets of the same configuration. Although the two doublets belong to the same configuration, the angular momenta couplings for the two pairs of chiral partners are different. This fact is reflected by the different alignment properties of the two doublets. The quasiparticle

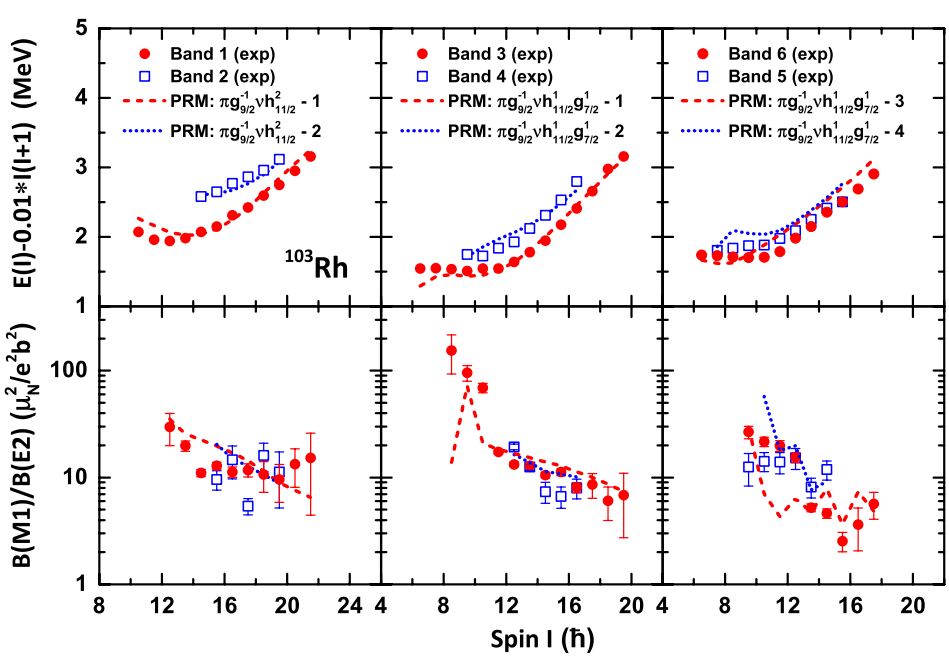

FIG. 4 (color online). Experimental excitation energies and $B(M1)/B(E2)$ ratios for the positive-parity chiral bands 1–2 (left panels) and negative-parity multiple chiral bands 3–6 (middle and right panels) in ^{103}Rh together with the results of the triaxial particle rotor model. The number following the configuration label of the theoretical curve corresponds to the energy ordering of the calculated band with the given configuration.

alignments are extracted from the calculated energy spectra by using the same experimental Harris parameters for bands 3–6. It can be seen that the calculated alignments to some extent are in agreement with the experimental values. The sharp increase of alignments around $\hbar\omega = 0.45$ MeV for bands 5, 6 are not reproduced, which might be attributed to a frozen core used in the framework of the particle rotor model. The theoretical alignment shows a smooth increasing rather than a sharp increasing. Observation of MχD with the same configuration shows that the chiral geometry in nuclei can be robust against the increase of the intrinsic excitation energy.

In summary, one positive-parity and two negative-parity chiral doublet band structures have been identified in ^{103}Rh. The observed doublet bands have been compared with results of calculations involving adiabatic and configuration-fixed constrained CDFT, TAC-CDFT, and the quantum particle rotor model. The theoretical results reproduce the data rather well. According to these results, the positive-parity doublet has a chiral vibrational structure based on the $\pi(1g_{9/2})^{-1} \otimes \nu(1h_{11/2})^2$ configuration, while the two negative-parity doublets are chiral doublets with the same $\pi(1g_{9/2})^{-1} \otimes \nu(1h_{11/2})^1(1g_{7/2})^1$ configuration. It provides the first experimental evidence for the MχD with the same configuration and shows that chiral geometry can be robust against the increase of the intrinsic excitation energy.

We thank the crew and staff of the 88-inch cyclotron. Special thanks to A. O. Macchiavelli and I. Y. Lee for their help in the experiment. This work was supported in part by the Hungarian Scientific Research Fund, OTKA (Contract No. K100835), the Major State 973 Program of China (Grant No. 2013CB834400), the National Natural Science Foundation of China (Grants No. 11175002, No. 11335002, and No. 11375015), the Research Fund for the Doctoral Program of Higher Education (Grant No. 20110001110087), the China Postdoctoral Science Foundation (Grants No. 2012M520101 and No. 2013M540011), the Natural Sciences and Engineering Research Council of Canada under Contract No. SAPIN/371656-2010, and the UK Engineering and Physical Sciences Research Council.

[1] S. Frauendorf and J. Meng, Nucl. Phys. **A617**, 131 (1997).
[2] K. Starosta *et al.*, Phys. Rev. Lett. **86**, 971 (2001).
[3] A. A. Hecht *et al.*, Phys. Rev. C **63**, 051302(R) (2001).
[4] D. J. Hartley *et al.*, Phys. Rev. C **64**, 031304(R) (2001).
[5] T. Koike, K. Starosta, C. J. Chiara, D. B. Fossan, and D. R. LaFosse, Phys. Rev. C **63**, 061304(R) (2001).
[6] R. A. Bark, A. M. Baxter, A. P. Byrne, G. D. Dracoulis, T. Kibédi, T. R. McGoram, and S. M. Mullins, Nucl. Phys. **A691**, 577 (2001).
[7] K. Starosta, C. J. Chiara, D. B. Fossan, T. Koike, T. T. S. Kuo, D. R. LaFosse, S. G. Rohozinski, Ch. Droste, T. Morek, and J. Srebrny, Phys. Rev. C **65**, 044328 (2002).
[8] T. Koike, K. Starosta, C. J. Chiara, D. B. Fossan, and D. R. LaFosse, Phys. Rev. C **67**, 044319 (2003).
[9] G. Rainovski *et al.*, Phys. Rev. C **68**, 024318 (2003).
[10] S. Zhu *et al.*, Phys. Rev. Lett. **91**, 132501 (2003).
[11] H. C. Jain, S. Lakshmi, and P. K. Joshi, AIP Conf. Proc. **764**, 99 (2005).
[12] J. Srebrny, E. Grodner, T. Morek, I. Zalewska, Ch. Droste, J. Mierzejewski, A. A. Pasternak, J. Kownacki, and J. Perkowski, Acta Phys. Pol. **36**, 1063 (2005).
[13] E. Grodner *et al.*, Phys. Rev. Lett. **97**, 172501 (2006).
[14] C. Vaman, D. B. Fossan, T. Koike, K. Starosta, I. Y. Lee, and A. O. Macchiavelli, Phys. Rev. Lett. **92**, 032501 (2004).
[15] P. Joshi *et al.*, Phys. Lett. B **595**, 135 (2004).
[16] P. Joshi *et al.*, Eur. Phys. J. A **24**, 23 (2005).
[17] J. A. Alcántara-Núñez *et al.*, Phys. Rev. C **69**, 024317 (2004).
[18] J. Timár *et al.*, Phys. Lett. B **598**, 178 (2004).
[19] J. Timár, C. Vaman, K. Starosta, D. B. Fossan, T. Koike, D. Sohler, I. Y. Lee, and A. O. Macchiavelli, Phys. Rev. C **73**, 011301(R) (2006).
[20] D. L. Balabanski *et al.*, Phys. Rev. C **70**, 044305 (2004).
[21] S. Y. Wang *et al.*, Phys. Lett. B **703**, 40 (2011).
[22] J. Meng, J. Peng, S. Q. Zhang, and S.-G. Zhou, Phys. Rev. C **73**, 037303 (2006).
[23] J. Peng, H. Sagawa, S. Q. Zhang, J. M. Yao, Y. Zhang, and J. Meng, Phys. Rev. C **77**, 024309 (2008).
[24] J. M. Yao, B. Qi, S. Q. Zhang, J. Peng, S. Y. Wang, and J. Meng, Phys. Rev. C **79**, 067302 (2009).
[25] J. Li, S. Q. Zhang, and J. Meng, Phys. Rev. C **83**, 037301 (2011).
[26] A. D. Ayangeakaa *et al.*, Phys. Rev. Lett. **110**, 172504 (2013).
[27] B. Qi, H. Jia, N. B. Zhang, C. Liu, and S. Y. Wang, Phys. Rev. C **88**, 027302 (2013).
[28] C. Droste, S. G. Rohozinski, K. Starosta, L. Prochniak, and E. Grodner, Eur. Phys. J. A **42**, 79 (2009).
[29] Q. B. Chen, J. M. Yao, S. Q. Zhang, and B. Qi, Phys. Rev. C **82**, 067302 (2010).
[30] I. Hamamoto, Phys. Rev. C **88**, 024327 (2013).
[31] D. C. Radford, Nucl. Instrum. Methods Phys. Res., Sect. A **361** 297 (1995); , **361** 306 (1995); http://radware.phy.ornl.gov.
[32] H. Dejbakhsh, R. P. Schmitt, and G. Mouchaty, Phys. Rev. C **37**, 621 (1988).
[33] A. Krämer-Flecken, T. Morek, R. M. Lieder, W. Gast, G. Hebbinghaus, H. M. Jäger, and W. Urban, Nucl. Instrum. Methods Phys. Res., Sect. A **275**, 333 (1989); K. S. Krane, R. M. Steffen, and R. M. Wheeler, At. Data Nucl. Data Tables **11**, 351 (1973).
[34] R. Bengtsson and S. Frauendorf, Nucl. Phys. **A327**, 139 (1979).
[35] P. W. Zhao, S. Q. Zhang, J. Peng, H. Z. Liang, P. Ring, and J. Meng, Phys. Lett. B **699**, 181 (2011).
[36] P. W. Zhao, J. Peng, H. Z. Liang, P. Ring, and J. Meng, Phys. Rev. Lett. **107**, 122501 (2011).
[37] P. W. Zhao, J. Peng, H. Z. Liang, P. Ring, and J. Meng, Phys. Rev. C **85**, 054310 (2012).
[38] J. Meng, J. Peng, S. Q. Zhang, and P. W. Zhao, Front. Phys. **8**, 55 (2013).
[39] B. Qi, S. Q. Zhang, J. Meng, S. Y. Wang, and S. Frauendorf, Phys. Lett. B **675**, 175 (2009).
[40] B. Qi, S. Q. Zhang, S. Y. Wang, J. Meng, and T. Koike, Phys. Rev. C **83**, 034303 (2011).
[41] P. W. Zhao, Z. P. Li, J. M. Yao, and J. Meng, Phys. Rev. C **82**, 054319 (2010).
[42] S. Y. Wang, B. Qi, and S. Q. Zhang, Chin. Phys. Lett. **26**, 052102 (2009).
[43] B. Qi, S. Q. Zhang, S. Y. Wang, J. M. Yao, and J. Meng, Phys. Rev. C **79**, 041302(R) (2009).